Hydrogen storage capacities of nanoporous carbon calculated by density functional and Møller-Plesset methods

I. Cabria,[1] M. J. López,[1] and J. A. Alonso[1,2]
[1]*Departamento de Física Teórica, Atómica y Óptica, Universidad de Valladolid, 47005 Valladolid, Spain*
[2]*Donostia International Physics Center (DIPC), 20018 San Sebastián, Spain*
(Received 11 May 2008; revised manuscript received 9 July 2008; published 13 August 2008)

The hydrogen storage capacities of nanoporous carbons, simulated as flat graphene slit pores, have been calculated using a quantum-thermodynamical model. The model is applied for several interaction potentials between the hydrogen molecules and the graphitic walls that have been generated from density functional theory (DFT) and second-order Møller-Plesset (MP2) calculations. The hydrogen storage properties of the pores can be correlated with the features of the potential. It is shown that the storage capacity increases with the depth of the potential, D_e. Moreover, the optimal pore widths, yielding the maximum hydrogen storage capacities, are close to twice the equilibrium distance of the hydrogen molecule to one graphene layer. The experimental hydrogen storage capacities of several nanoporous carbons such as activated carbons (ACs) and carbide-derived carbons (CDCs) are well reproduced within the slit pore model considering pore widths of about 4.9–5.1 Å for the DFT potential and slightly larger pore widths (5.3–5.9 Å) for the MP2 potentials. The calculations predict that nanoporous carbons made of slit pores with average widths of 5.8–6.5 Å would yield the highest hydrogen storage capacities at 300 K and 10 MPa.

DOI: 10.1103/PhysRevB.78.075415 PACS number(s): 68.43.−h, 84.60.Ve, 73.22.−f

I. INTRODUCTION

The targets of the hydrogen storage capacities for the year 2010 that would permit the use of hydrogen as a fuel in on-board automotive applications are at least 6% of the storage system weight and more than 0.045 kg of hydrogen per liter.[1,2] With these targets fulfilled, the hydrogen cars would have the same autonomy range as that of the present gasoline cars. One of the proposed ways to store hydrogen is based on the physisorption of molecular hydrogen on low weight materials with a large specific surface area, such as carbon nanotubes (CNTs) and porous carbons. Recent reviews[3–5] concluded that the hydrogen storage capacity of CNTs is very small (less than 1 wt %) at room temperature and moderate pressures and that CNTs are not superior to other carbon nanostructures for hydrogen storage. Theoretical calculations yield binding energies of H_2 on graphite, graphene,[6–9] and CNTs (Refs. 8 and 10–14) between 70 and 100 meV, in reasonable agreement with the experimental results, which have a large dispersion of values, between 20 and 110 meV.[15–18] A guide to designing graphitic materials that would reach the hydrogen storage targets is provided by the thermodynamical analysis of Li *et al.*[12] They estimated that a binding energy of 300–400 meV/molecule would be required for reversible adsorption/desorption at room temperature and normal pressures.

Nanoporous carbons are promising materials for hydrogen storage due to their porosity, low weight, and large specific area, and recent experiments confirmed this expectation.[19–29] In a previous paper[30,31] we investigated the hydrogen storage capacity of nanoporous carbons[32,33] by applying a quantum-thermodynamical model.[30,34] The nanopores were simulated as graphene slit pores consisting of two parallel flat graphene layers separated by a certain distance or width. The interaction potential between a hydrogen molecule and a graphene layer was generated from density functional theory (DFT) calculations using the local-density approximation (LDA).[35] The quantum-thermodynamical model explains the experimental storage capacities of activated carbons (ACs) (Refs. 20 and 26) and carbide-derived carbons (CDCs) (Refs. 19, 23, and 24) and allows making interesting predictions about the optimum nanopore size.

Clearly, the results of the quantum-thermodynamical model depend on the interaction potential between the hydrogen molecules and the pore walls. However, it is not easy to guess *a priori* the effect that changing the interaction potential will produce in the predicted storage capacities of the pores. In this paper we analyze different models for the interaction potential and the corresponding storage capacities. A useful approach for calculating the potential energy of the hydrogen molecule inside the slit pore consists of summing up the interaction potentials of the molecule with each individual graphene layer. This is the additive approach that has to be compared with the exact procedure, in which the potential energy is calculated directly for the hydrogen molecule inside the slit pore interacting with the two graphene walls at the same time. In Sec. II we compare the results obtained with the additive approach and the exact procedure using in both cases the DFT-LDA formalism to calculate the potentials. On the other hand, there is some debate in the scientific community concerning the description of weak intermolecular interactions using DFT methods. This applies, in particular, to the description of the adsorption of molecular hydrogen on graphitic surfaces. To shed some light on this debate, we have compared the interaction potentials between H_2 and graphene calculated using the DFT-LDA approach and the quantum-mechanical second-order Møller-Plesset (MP2) method.[36] These potentials are then used in the thermodynamical model and the predicted hydrogen storage capacities are compared and discussed in Sec. III. The two models are also compared with the experimental hydrogen storage capacities of ACs and CDCs. We finish with the conclusions in Sec. IV.

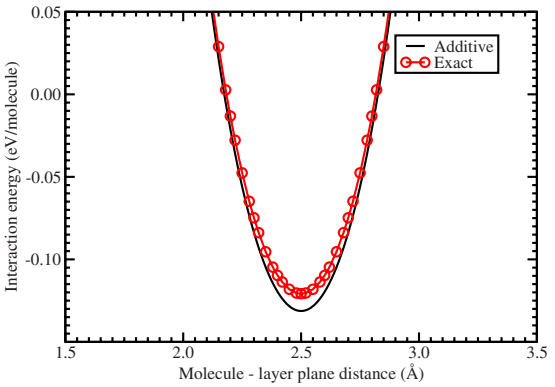

FIG. 1. (Color online) Potential energy of a hydrogen molecule inside a slit pore of 5 Å width as a function of the distance between the molecule and the left wall. The exact potential and the additive approach are calculated using the DFT-LDA formalism.

II. ADDITIVE APPROACH

A carbon slit pore consists of two parallel flat graphene layers at a distance d. The interaction potential felt by a hydrogen molecule inside the slit pore can be approximated by the sum of the interactions of the molecule with each of the pore walls, independently. This is called the additive approach. For a molecule inside the slit pore at a distance z from the first graphene layer and at a distance $d-z$ from the second layer, the additive potential is given by $V(z)+V(d-z)$, where V is the interaction potential with one graphene layer. Note that the potential V is calculated only once and can be used for pores of any width. This additive approach was used in Refs. 30 and 34. The exact potential, on the other hand, is obtained from calculations in which the molecule interacts with the two pore walls at the same time, and it has to be recalculated for each pore width d. The additive approach is expected to be very accurate for large pores in which the two graphene layers are far apart. However for smaller pore sizes (on the order of two times the equilibrium distance of the hydrogen molecule to one graphene layer), the additive approach is less accurate since the two layers begin to interact and the presence of one wall modifies the interaction of the hydrogen molecule with the other wall, and vice versa.

Figure 1 shows the exact and the additive potential energies of a hydrogen molecule inside a slit pore of 5 Å width. Both potentials have been calculated using the DFT-LDA formalism[35] as implemented in the DACAPO code.[37,38] The two graphene layers of the slit pore are placed on registry and the hydrogen molecule is placed above the center of a carbon hexagon of one of the graphene layers with the molecular axis perpendicular to the graphene plane. For this narrow pore, the two potentials have a single minimum at the center of the slit pore. The potential depths are 0.121 and 0.131 eV/molecule for the exact and additive potentials, respectively. The difference between the exact and the approximated potentials is significant only in the range of distances $z=2.25-2.75$ Å and decreases very fast when the molecule departs from the center of the slit pore, as can be seen in Fig. 1.

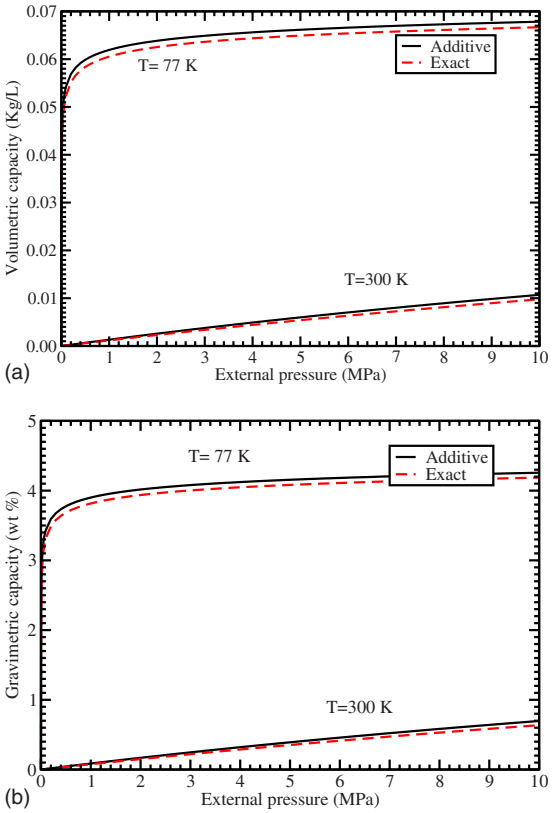

FIG. 2. (Color online) Excess volumetric (in kilograms of hydrogen per liter) and gravimetric (in hydrogen weight percent of total weight of the storage system) hydrogen storage capacities of carbon slit pores of 5 Å width at 77 and 300 K as a function of pressure. Comparison of the results obtained using the additive approach and the exact interaction potentials.

We have applied the quantum-thermodynamical model introduced in Ref. 30 to calculate the hydrogen storage capacity of the 5-Å-wide slit pore. Each of the two DFT-LDA interaction potentials, the exact and the additive, shown in Fig. 1, are used in the first step of the thermodynamical model to calculate the quantum states of the hydrogen molecule inside the pore. Then, the equilibrium constant between the hydrogen physisorbed and the nonadsorbed molecules (compressed externally) is obtained from the quantum states of the molecule. Finally, the gravimetric and volumetric capacities are calculated from the equilibrium constant and the equation of state of hydrogen. Figures 2 and 3 compare the storage capacities of the 5-Å-wide slit pore as a function of external pressure and temperature, respectively, obtained using the exact and additive potentials. The differences between the results of the two potentials are very small. The largest relative difference of about 20% appears in the region of low temperatures and low pressures. Our conclusion is that the additive approach is sufficiently accurate compared to the exact potential and can be used to predict the storage capacity of nanoporous carbons.

III. MP2 AND DFT INTERACTION POTENTIALS

There is some debate about the use of DFT methods for investigating the physisorption of molecular hydrogen on

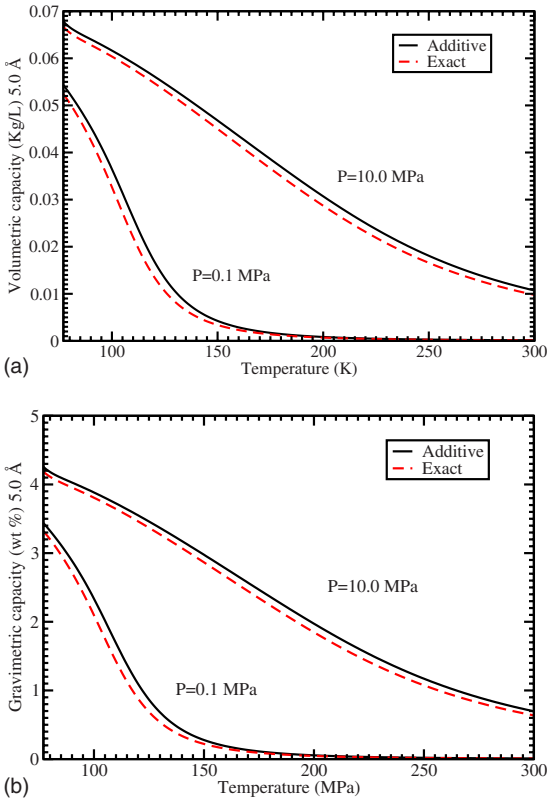

FIG. 3. (Color online) The same as Fig. 2 at pressures of 0.1 and 10 MPa and as a function of temperature.

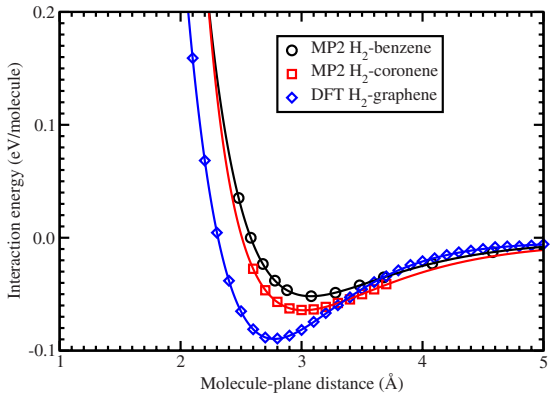

FIG. 4. (Color online) Interaction potentials $V(z)$ of a single hydrogen molecule with benzene, C_6H_6, and coronene, $C_{24}H_{12}$, calculated using the high level MP2 method (Refs. 41 and 42, respectively), and interaction potential between a hydrogen molecule and a graphene layer, calculated using the DFT-LDA formalism. The potentials are given as a function of the distance z between the hydrogen molecule and the plane of the graphene (benzene, coronene).

graphitic-type surfaces. It is known that the usual DFT approximations [LDA, generalized gradient approximation (GGA)] do not include explicitly the long-range dispersion forces. However, there is evidence that the LDA reproduces reasonably well the potential-energy curve around the equilibrium separation for the interaction between two graphitic systems[39] or between molecular hydrogen and a graphitic wall.[6,11] The LDA binding energy arises in those cases from exchange-correlation effects between the overlapping electron densities and from a small redistribution of the electronic density.[6,11] Although the dispersive long-range limit of the interaction potential is not captured by the LDA, this is not a big drawback when investigating the adsorption of H_2 molecules since only the values of the interaction potential around the equilibrium configuration are relevant. This explains the success of the DFT-LDA formalism in investigations of the hydrogen physisorption in carbonaceous materials. Previous studies[6–9,11–14] showed that the LDA predicts the adsorption energies of H_2 on the surface of graphite and carbon nanotubes in reasonable agreement with experiments.[15–18] On the other hand, the quantum-mechanical MP2 and coupled cluster (CC) methods take into account the dispersion forces and, for this reason, are usually considered as more accurate than DFT for studying physisorption problems. The disadvantage of the MP2 and CC methods is that they require much more memory resources and computation time than DFT. Therefore, they can be applied only to small systems. In an excellent paper Zhao and Truhlar[40] calculated the weak interactions in 28 small systems composed by couples of small molecules and/or atoms such as $(NH_3)_2$, $(HF)_2$, $C_2H_4\cdots F_2$, $HCl\cdots H_2S$, $CH_4\cdots Ne$, and $C_6H_6\cdots Ne$, among others. The authors compared the results of 44 different DFT functionals and the results of the MP2 method and concluded that the DFT methods are valid tools for studying weak interactions.[40]

Since the MP2 method is too expensive to be applied to large systems, some cluster models such as benzene and the $C_{24}H_{12}$ planar coronene are usually considered to mimic an infinitely large graphene layer. Several authors[34,41] calculated, using the MP2 methodology, the interaction of one

TABLE I. Potential depth D_e (in eV) and equilibrium distance r_e (in Å) of molecular hydrogen physisorbed on graphitic walls as calculated from the DFT H_2-graphene, MP2 H_2-coronene, and MP2 H_2-benzene potentials. The optimal slit pore width d_{opt} (in Å) for hydrogen adsorption and the corresponding maximum volumetric v_c (in kg H_2/L) and gravimetric g_c (in wt %) storage capacities are given for those potentials at a pressure of 10 MPa and temperatures of 77 K and 300 K.

			77 K, 10 MPa		300 K, 10 MPa		
Type	D_e	r_e	d_{opt}	v_c	d_{opt}	v_c	g_c
DFT H_2-graphene	0.089	2.80	6.0	0.097	5.8	0.043	3.19
MP2 H_2-coronene	0.064	3.00	6.6	0.090	6.4	0.025	2.09
MP2 H_2-benzene	0.052	3.10	6.7	0.083	6.5	0.015	1.28

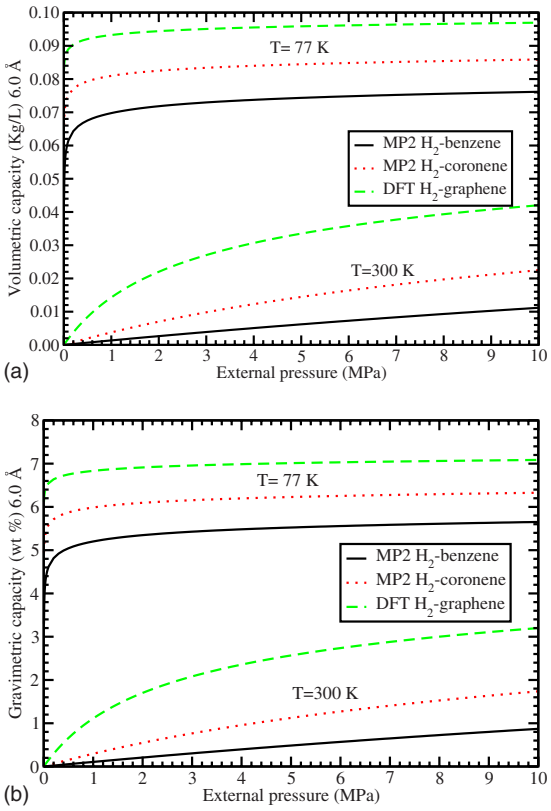

FIG. 5. (Color online) Excess hydrogen volumetric and gravimetric storage capacities of carbon slit pores of 6 Å width as a function of the external pressure. The solid, dotted, and dashed lines correspond to the results obtained using the MP2 H_2-benzene, the MP2 H_2-coronene, and the DFT H_2-graphene interaction potentials, respectively, introduced in Sec. III.

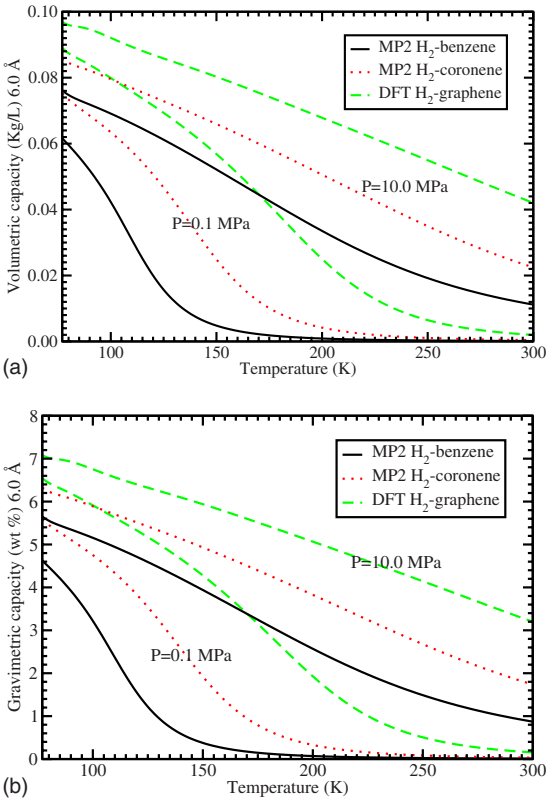

FIG. 6. (Color online) Excess hydrogen volumetric and gravimetric storage capacities of carbon slit pores of 6 Å width as a function of temperature. The solid, dotted, and dashed lines correspond to the results obtained using the MP2 H_2-benzene, the MP2 H_2-coronene, and the DFT-LDA H_2-graphene interaction potentials, respectively, introduced in Sec. III. The upper curves give the storage capacities at a pressure of 10 MPa and the lower curves at 0.1 MPa.

hydrogen molecule with benzene. The H_2 molecule was placed above the center of the hexagonal C ring of benzene with its axis perpendicular to the ring. The MP2 calculations by Donchev[41] were performed using the aug-cc-PVTZ basis functions for all the atoms and corrected for the basis set superposition error (BSSE). The interaction potential as a function of the distance between the two molecules, MP2 H_2-benzene potential, is given in Fig. 4. Okamoto and Miyamoto[7] compared DFT-LDA and MP2 calculations of the adsorption of a hydrogen molecule on the $C_{24}H_{12}$ coronene. The two sets of results were in good agreement, giving a binding energy of 0.086 eV/molecule at an equilibrium distance of 3 Å, but the MP2 calculations ignored the BSSE. Ferre-Vilaplana[42] performed analogous MP2 calculations correcting the energies by BSSE (Ref. 43) and found a binding energy of 0.037 eV/molecule and an equilibrium separation of 3.2 Å. However, using a basis set of higher quality, the aug-cc-PVTZ basis functions for the hydrogen molecule and the six closest carbon atoms and cc-PVTZ basis functions for the rest of atoms, he obtained a binding energy of 0.064 eV/molecule at the equilibrium separation of 3.0 Å. We call this last high quality MP2 interaction potential between the H_2 molecule and the coronene, the MP2 H_2-coronene potential. This potential is plotted in Fig. 4. The accuracy of the MP2 results depends on details of the calculations such as the selected basis set and the BSSE corrections. The MP2 calculations selected here for the interactions between H_2 and benzene[41] and between H_2 and the coronene[42] are of high accuracy. One should bear in mind, however, that these potentials are obtained for model systems and not for the graphene layer. Nowadays a MP2 calculation for H_2 interacting with an infinite graphene layer is practically unfeasible because of the high memory resources and computation time required.

DFT-GGA calculations using the PW91 functional[44] performed by Tada *et al.*[45] yielded repulsive interactions between H_2 and a graphene layer and also between H_2 and a (6,6) nanotube. However, in previous papers[11,13,14] we showed that the DFT-LDA formalism leads to adsorption binding energies of H_2 on the external surface of carbon nanotubes consistent with the MP2 results. The hydrogen adsorption energy on a (4,4) nanotube is about 80 meV/molecule. We have calculated the interaction potential between H_2 and a graphene layer using the DFT-LDA formalism. We name it the DFT H_2-graphene potential and plot it in Fig. 4. Comparison of the three potentials plotted in Fig. 4 shows that the potential-well depth D_e increases from MP2 H_2-benzene to MP2 H_2-coronene to DFT H_2-graphene, whereas the equilibrium potential distance r_e decreases in the same sequence. The values of D_e and r_e for the three poten-

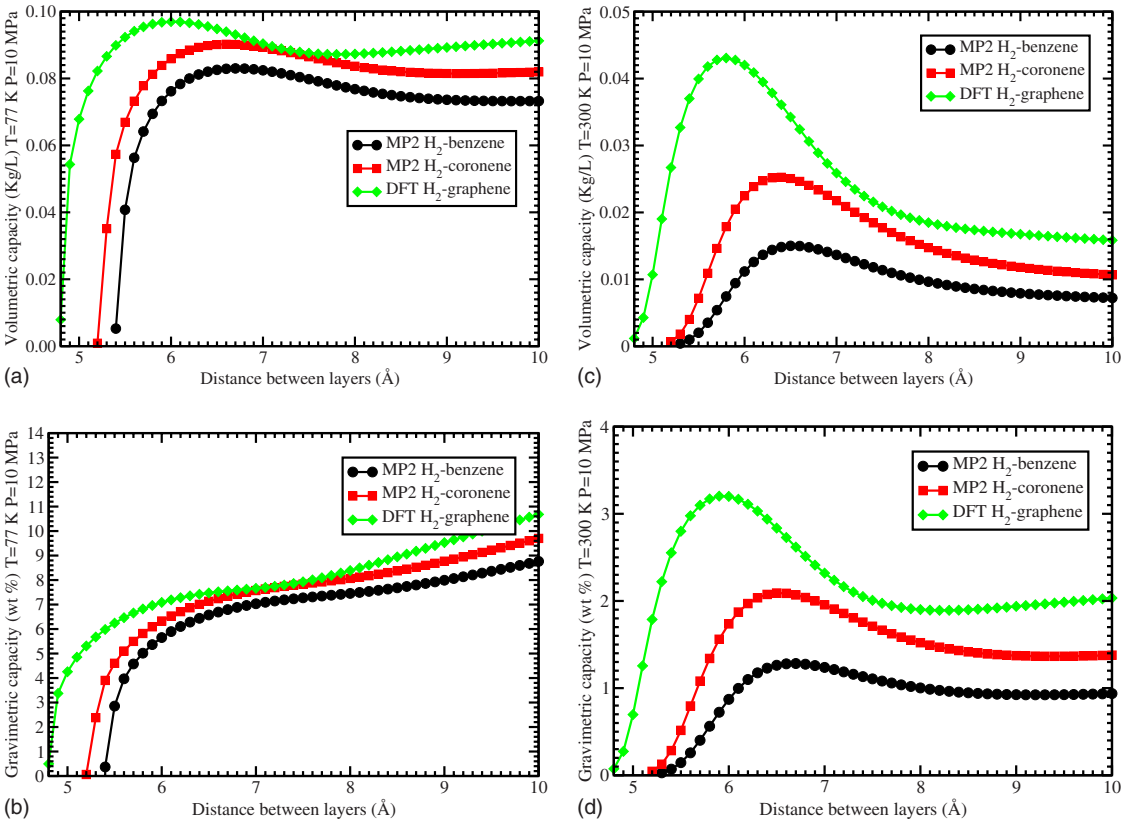

FIG. 7. (Color online) Excess hydrogen volumetric and gravimetric storage capacities of carbon slit pores as a function of pore width. The circles, squares, and diamonds correspond to the results obtained using the MP2 H_2-benzene, the MP2 H_2-coronene, and the DFT H_2-graphene interaction potentials, respectively, introduced in Sec. III. The left panels give the storage capacities at 10 MPa and 77 K and the right panels those at 10 MPa and 300 K.

tials are given in Table I. Obviously, the differences between the potentials will have consequences in the hydrogen storage properties of slit pores calculated using those potentials.

For the range of molecule-plane distances of interest for our calculations, the H-H bond length remains unaltered by the interaction with the graphitic surfaces. Actually, in a previous work[11] we found that for molecule-surface distances larger than 1.62 Å there is practically no relaxation of the bond length of the H_2 molecule.

IV. MP2 AND DFT HYDROGEN STORAGE CAPACITIES

A. Comparison of the theoretical capacities

In this subsection we compare the slit pore hydrogen storage capacities predicted by the quantum-thermodynamical model described in Sec. II using the two MP2 and the DFT-LDA interaction potentials between H_2 and graphitic walls introduced in Sec. III. For the three potentials we use the additive approach, $V(z)+V(d-z)$, to calculate the potential energy of a hydrogen molecule inside the slit pore. The volumetric and gravimetric capacities of slit pores of 6 Å width are shown in Figs. 5 and 6 as a function of external pressure and temperature, respectively. The three potentials yield the same overall shape of the hydrogen storage capacities as a function of external pressure and temperature. Figure 5 shows that, as expected, the hydrogen storage capacities are increasing functions of the external pressure. One should note, however, that at low temperatures ($T=77$ K) the storage capacities saturate and tend to a constant value already for moderate pressures ($\sim$1 MPa), in agreement with the experimental results.[26] In contrast, at room temperature the capacities do not saturate and become almost linear functions at pressures of about 4 MPa. On the other hand, the storage capacities decrease with increasing temperature, as shown in Fig. 6. At atmospheric pressure (0.1 MPa) the decrease is quite steep, whereas at high pressure (10 MPa) the capacities decrease almost linearly with temperature. At room temperature (300 K) and atmospheric pressure (0.1 MPa), the storage capacities are very small. The highest storage capacities are obtained at low temperature (77 K) and high pressure (10 MPa).

The DFT-LDA based potential produces higher storage capacities than the two MP2 based potentials. This correlates with the larger binding energy of H_2 to the graphitic wall obtained with the DFT-LDA formalism. The differences between the hydrogen storage capacities obtained with the DFT-LDA and the two MP2 potentials increase linearly with the external pressure at 300 K but are almost constant at 77 K (0.01 kg H_2/L and 0.6 wt % differences between the DFT H_2-graphene and the MP2 H_2-coronene results and 0.02 kg H_2/L and 1.2 wt % differences between the DFT H_2-graphene and the MP2 H_2-benzene results). At a pressure of 10 MPa the differences are larger (by a factor of about

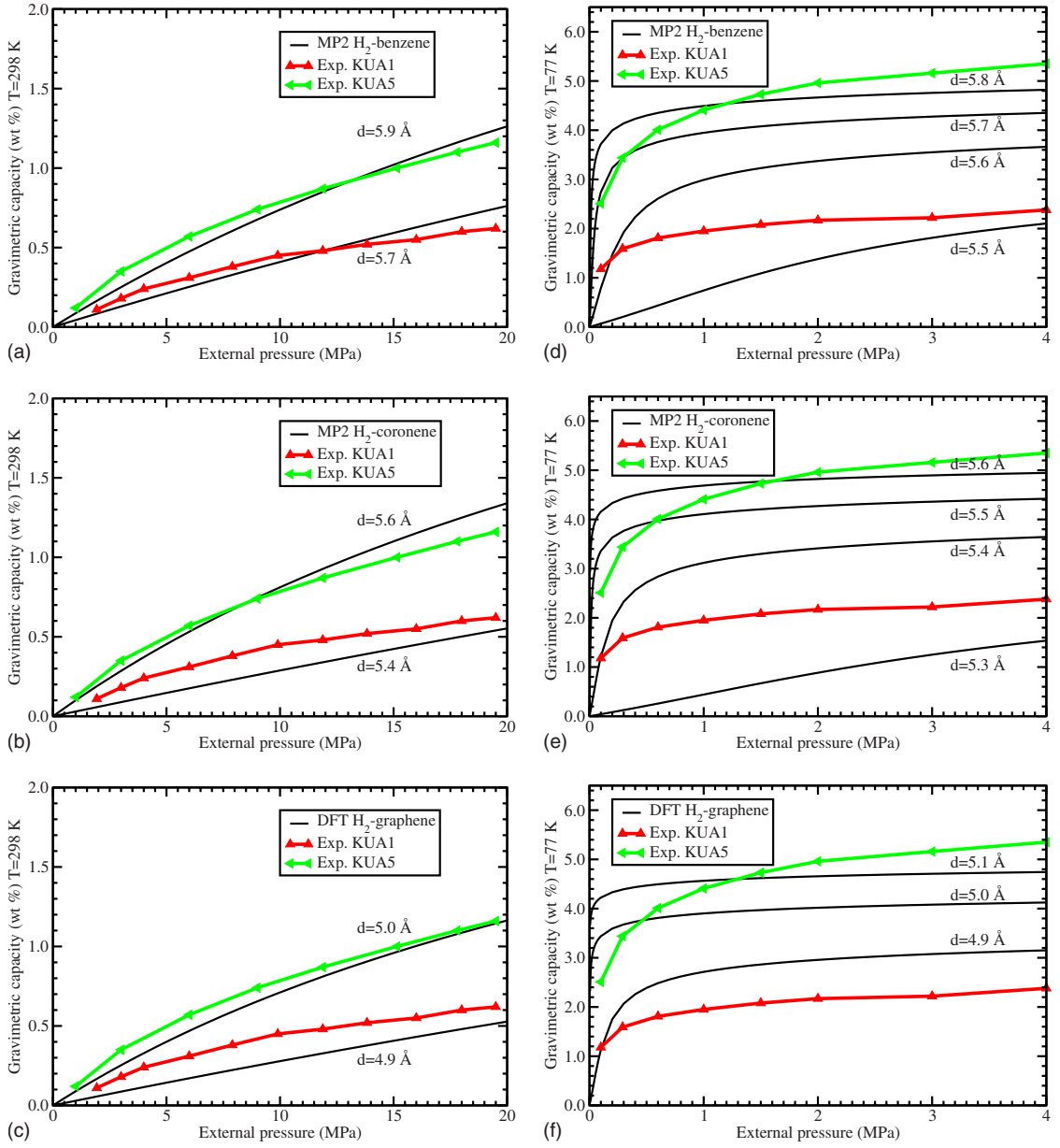

FIG. 8. (Color online) Excess hydrogen gravimetric storage capacities of two samples of ACs (named KUA1 and KUA5) measured by Jordá-Beneyto *et al.* (Ref. 26) as a function of pressure at 298 K (left panels) and 77 K (right panels). The theoretical capacities for those slit pore widths that fit the experiment better are plotted for each of the three interaction potentials investigated in this paper in the different panels.

1.5) for 300 K than for 77 K, and those differences as a function of temperature are larger at 0.1 MPa than at 10 MPa.

It is interesting to investigate the dependence of the hydrogen storage capacities on the slit pore width d. Figure 7 shows for a pressure of 10 MPa and the temperatures of 77 and 300 K that the three interaction potentials considered lead to a similar behavior of the capacities as a function of pore width, although differences in the absolute capacities are apparent. At 300 K both the volumetric and the gravimetric capacities exhibit a maximum as a function of pore width. However, at low temperatures (77 K) only the volumetric capacity has a maximum, whereas the gravimetric capacity is an increasing function of the pore width. The position of the maxima correspond to the optimal pore widths d_{opt} for hydrogen storage under the given conditions. This optimal pore width d_{opt} is sensitive to the interaction potential used in the calculations. The maximum volumetric capacity at 300 K and 10 MPa is obtained for pore widths of 5.8, 6.4, and 6.5 Å for the DFT H_2-graphene, MP2 H_2-coronene, and MP2 H_2-benzene potentials, respectively. The maximum gravimetric capacities are reached for pore sizes 0.1 Å larger than those corresponding to the maximum volumetric capacities. At 77 K and 10 MPa the volumetric capacities reach a maximum at pore widths of 6.0, 6.6, and 6.7 Å for the previous potentials, respectively. The differences between the storage capacities obtained with the DFT-LDA and the two MP2-type interaction potentials are larger at high tempera-

ture (300 K). The data of the optimum pore widths and the corresponding maximum storage capacities are compiled in Table I.

The optimal pore width is a little larger than two times the equilibrium distance r_e of hydrogen to the graphitic wall for the corresponding interaction potential. This indicates that for the pore width d_{opt}, the hydrogen molecules are optimally encaged within the pore. That is, they maximize their interactions with the two walls of the pore. Increasing the pore width above d_{opt} reduces the interaction of the hydrogen molecules with the pore walls, and eventually the molecules interact mainly with one of the walls of the pore. At high (300 K) temperatures, the hydrogen uptake in the pore soon reaches a saturation value (corresponding to the hydrogen uptake in the isolated walls). Therefore, the volumetric capacity decreases with increasing pore width due to the linear increase in the pore volume. The behavior at low (77 K) temperature is different. Despite the lowering of the interaction energy with increasing pore width, the gravimetric capacity increases. This is because the thermal energy of the molecules is small. Therefore, as the pore width increases, more and more molecules adsorb in the pore walls under the action of the interaction potential and the external pressure. The increase in the amount of adsorbed hydrogen tends to compensate the linear increase in the pore volume and, as a result, the volumetric capacity first decreases and then recovers to a constant value smaller than the maximum capacity.

We have shown in this subsection that the volumetric and gravimetric hydrogen storage capacities of slit pores depend on which interaction potential between the hydrogen molecules and the graphitic walls is used in the calculations. The highest capacities are obtained for the DFT H_2-graphene potential and the smallest ones for the MP2 H_2-benzene potential. For each potential, the maximum capacity is reached for pores with the optimal width d_{opt}. The optimal width follows the same trend as the equilibrium distance r_e of the potential: It has the smaller value for the DFT H_2-graphene potential and the largest value for the MP2 H_2-benzene potential (see Table I). On the other hand, the maximum storage capacities are proportional to the potential-well depth D_e. Qualitatively one can understand the dependence of the storage capacities on the D_e and r_e parameters of the interaction potential of hydrogen with a graphitic wall. A deeper potential well leads to a stronger interaction. The quantum-mechanical molecular levels in a deeper potential (assuming similar width) are more profound. Therefore, the equilibrium of the adsorbed molecules in that potential with the externally compressed gas displaces toward the adsorbed phase giving rise to higher storage capacities.

B. Comparison with experiments

Challet *et al.*[20] measured the hydrogen storage capacity of activated carbons with an average porous size of about 5 Å. At 77 K and saturation pressure (about 3 MPa), they found a gravimetric capacity of almost 2.5 wt %. The quantum-mechanical calculations of slit pores match this experimental value considering pore widths of 4.95, 5.35, and 5.5 Å for the DFT H_2-graphene, MP2 H_2-coronene, and the MP2 H_2-benzene potentials, respectively. This result seems to indicate slightly better agreement of the DFT H_2-graphene model with this experiment.

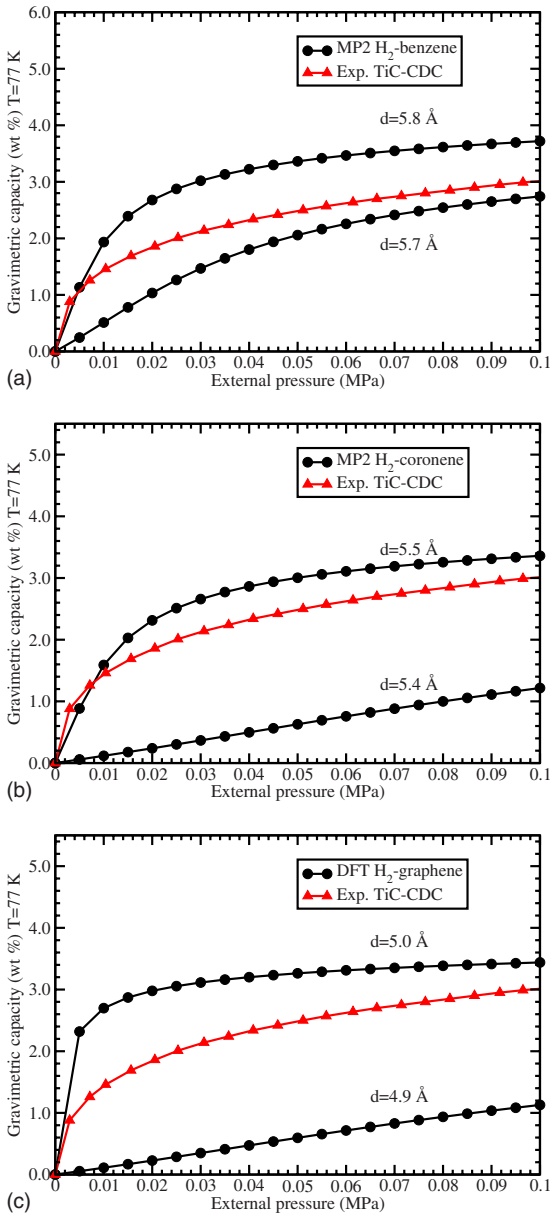

FIG. 9. (Color online) Excess hydrogen gravimetric storage capacity of CDCs derived from TiC measured by Gogotsi *et al.* (Ref. 23) as a function of pressure at 77 K. The theoretical capacities for those slit pore widths that fit the experiment better are plotted for each of the three interaction potentials investigated in this paper in the different panels.

The gravimetric storage capacities measured by Jordá-Beneyto *et al.*[26] for two samples of activated carbons, named KUA1 and KUA5, as a function of pressure at $T=77$ and 298 K are given in Fig. 8. Independent measurements by Terrés *et al.*[21] and Panella *et al.*,[22] among others, on different samples of activated carbons lay between the experimental curves for the samples KUA1 and KUA5 given in the figure. The experimental capacities are compared with the calculated capacities within the slit pore model for the DFT

H_2-graphene, MP2 H_2-coronene, and the MP2 H_2-benzene potentials in different panels of Fig. 8. Since the pore size of the experimental samples is not known, the theoretical capacities are plotted for each potential for those values of the pore width that adjust better to the experimental curves. The experiments are well reproduced using pore widths between 4.9 and 5.9 Å. Figure 9 shows the comparison of the experimental[23] and the calculated gravimetric storage capacities at 77 K of CDCs obtained from TiC. The theoretical results are plotted for the two values of the pore width that fit the experiment better for each of the three potentials. The values of the pore width that adjust the experiment are similar to those obtained for CDCs. One should note, however, that the different potentials produce pore widths that are a little different. The DFT H_2-graphene potential, which is the strongest potential and has the smallest equilibrium distance r_e, predicts the smallest pore sizes of the samples. One has to take into account also that the real porous carbons, ACs and CDCs, contain pores of different shapes (planar, cylindrical, spherical, and others) and sizes. These effects should be considered to obtain better theoretical estimations of the storage capacities of nanoporous materials.

V. SUMMARY AND CONCLUSIONS

We have calculated the hydrogen storage capacities of nanoporous carbons applying a quantum-thermodynamical model to graphene slit pores[30,34] that simulate the pores in the material. The model depends on the interaction potential between the hydrogen molecules and the graphitic walls of the slit pore. The DFT-LDA approach for describing the interaction of molecular hydrogen with a graphene layer, DFT H_2-graphene potential, is compared with the potentials obtained using the MP2 methodology between H_2 and benzene,[41] MP2 H_2-benzene, and between H_2 and the $C_{24}H_{12}$ coronene,[42] MP2 H_2-coronene. The DFT-LDA formalism leads to a deeper potential well and a smaller equilibrium distance of H_2 to the graphitic wall than the two MP2 potentials. The additive approach for the potential, consisting of calculating the interaction potential of the H_2 molecules within the slit pore as the sum of the interactions with each wall separately, has proved to be quite accurate even for narrow (~5 Å) pores.

The three potentials investigated lead to hydrogen storage capacities of the slit pores that are increasing functions of the external pressure at room temperature. At low temperature (~77 K), the storage capacities saturate at moderate pressures, in agreement with the experimental results. The highest hydrogen storage capacities of the slit pores are obtained for the DFT H_2-graphene potential and the smallest ones for the MP2 H_2-benzene potential. This result shows that the storage capacity increases with the well depth D_e of the interaction potential between H_2 and the pore walls. The optimal pore widths, yielding the maximum hydrogen storage capacities at 300 K and 10 MPa, are rather similar, 5.8, 6.4, and 6.5 Å for the DFT H_2-graphene, MP2 H_2-coronene, and MP2 H_2-benzene potentials, respectively. Those widths are close to twice the equilibrium distance of the hydrogen molecule to a graphene layer, for the corresponding potential.

The experimental hydrogen storage capacities of activated carbons[20–22,26] and carbide-derived carbons[23] are well reproduced within the slit pore model. The DFT H_2-graphene potential predicts, in agreement with the available experimental data[20] on nanoporous carbons, pore widths of about 4.9–5.1 Å. The MP2 potentials predict pore widths that are a little larger (about 5.3–5.9 Å) for the same materials. However, according to our calculations, the pores that would yield the maximum storage capacities are a little larger than those of the carbon materials used in the experiments. Therefore, our results suggest that by gaining control on the shape and size of the pores in nanoporous carbons, it would be possible to optimize (increase) the storage capacity of those materials.

ACKNOWLEDGMENTS

This work was supported by MEC of Spain (Grants No. MAT2004-23280-E and No. MAT2005-06544-C03-01), Junta de Castilla y León (Grant No. VA039A05), and the University of Valladolid. I.C. acknowledges support from MEC-FSE through the Ramón y Cajal Program. J.A.A. acknowledges the hospitality and support of Donostia International Physics Center.

[1] http://www1.eere.energy.gov/hydrogenandfuelcells/pdfs/freedomcar_targets_explanations.pdf
[2] Multi-Year Research, Development and Demonstration Plan: Planned Program Activities for 2003-2010: Technical Plan; U. S. Department of Energy; http://www.eere.energy.gov/hydrogenandfuelcells/mypp/pdfs/storage.pdf
[3] A. Züttel, Mater. Today **6**, 24 (2003).
[4] S. Orimo, A. Züttel, L. Schlapbach, G. Majer, T. Fukunaga, and H. Fujii, J. Appl. Crystallogr. **356**, 716 (2003).
[5] D. K. Ross, Vacuum **80**, 1084 (2006).
[6] J. S. Arellano, L. M. Molina, A. Rubio, and J. A. Alonso, J. Chem. Phys. **112**, 8114 (2000).
[7] Y. Okamoto and Y. Miyamoto, J. Phys. Chem. B **105**, 3470 (2001).
[8] J. Zhao, A. Buldum, J. Han, and J. P. Lu, Nanotechnology **13**, 195 (2002).
[9] N. Jacobson, B. Tegner, E. Schröder, P. Hyldgaard, and B. I. Lundqvist, Comput. Mater. Sci. **24**, 273 (2002).
[10] G. E. Froudakis, Nano Lett. **1**, 531 (2001).
[11] J. S. Arellano, L. M. Molina, A. Rubio, M. J. López, and J. A. Alonso, J. Chem. Phys. **117**, 2281 (2002).
[12] J. Li, T. Furuta, H. Goto, T. Ohashi, Y. Fujiwara, and S. Yip, J. Chem. Phys. **119**, 2376 (2003).
[13] I. Cabria, M. J. López, and J. A. Alonso, Eur. Phys. J. D **34**, 279 (2005).
[14] I. Cabria, M. J. López, and J. A. Alonso, J. Chem. Phys. **123**,

204721 (2005).
[15] C. M. Brown, T. Yildirim, D. A. Newmann, M. J. Heben, T. Gennett, A. C. Dillon, J. L. Alleman, and J. E. Fischer, Chem. Phys. Lett. **329**, 311 (2000).
[16] B. K. Pradhan, G. U. Sumanasekera, K. W. Adu, H. E. Romero, K. A. Williams, and P. C. Eklund, Physica B (Amsterdam) **323**, 115 (2002).
[17] B. K. Pradhan, A. R. Harutyunyan, D. Stojkovic, J. C. Grossman, P. Zhang, M. W. Cole, V. Crespi, H. Goto, J. Fujiwara, and P. C. Eklund, J. Mater. Res. **2209**, 17 (2002).
[18] D. G. Narehood, J. V. Pearce, P. C. Eklund, P. E. Sokol, R. E. Lechner, J. Pieper, J. R. D. Copley, and J. C. Cook, Phys. Rev. B **67**, 205409 (2003).
[19] Y. Gogotsi, A. Nikitin, H. Ye, W. Zhou, J. E. Fischer, B. Yi, H. C. Foley, and M. W. Barsoum, Nat. Mater. **2**, 591 (2003).
[20] S. Challet, P. Azaïs, R. J.-M. Pellenq, O. Isnard, J.-L. Soubeyroux, and L. Duclaux, J. Phys. Chem. Solids **65**, 541 (2004).
[21] E. Terrés, B. Panella, T. Hayashi, Y. A. Kim, M. Endo, J. M. Domínguez, M. Hirscher, H. Terrones, and M. Terrones, Chem. Phys. Lett. **403**, 363 (2005).
[22] B. Panella, M. Hirscher, and S. Roth, Carbon **43**, 2209 (2005).
[23] Y. Gogotsi, R. K. Dash, G. Yushin, T. Yildirim, G. Laudisio, and J. E. Fischer, J. Am. Chem. Soc. **127**, 16006 (2005).
[24] G. Yushin, R. Dash, J. Jagiello, J. E. Fischer, and Y. Gogotsi, Adv. Funct. Mater. **16**, 2288 (2006).
[25] Z. X. Yang, Y. D. Xia, X. Z. Sun, and R. Mokaya, J. Phys. Chem. B **110**, 18424 (2006).
[26] M. Jordá-Beneyto, F. Suárez-García, D. Lozano-Castelló, D. Cazorla-Amorós, and A. Linares-Solano, Carbon **45**, 293 (2007).
[27] B. J. Kim and S. J. Park, J. Colloid Interface Sci. **311**, 619 (2007).
[28] F. Ding, Y. Lin, P. O. Krasnov, and B. I. Yakobson, J. Chem. Phys. **127**, 164703 (2007).
[29] Y. S. Lee, Y. H. Kim, J. S. Hong, J. K. Suh, and G. J. Cho, Catal. Today **120**, 420 (2007).
[30] I. Cabria, M. J. López, and J. A. Alonso, Carbon **45**, 2649 (2007).
[31] Figure 8 of Ref. 30 contains two errors: the gravimetric capacities of Wang and Johnson [Q. Wang and J. K. Johnson, J. Chem. Phys. **110**, 577 (1999)] at 77 K should be about 3 and 7 wt % for slit pores of 6 and 9 Å width, respectively, instead of 0.2 and 0.5 wt %.
[32] The classification of pore size proposed by the IUPAC is divided into micropores, mesopores, and macropores, which are pores with effective widths $w<2$ nm, 2 nm$\leq w\leq$50 nm, and $w>50$ nm, respectively. We use the term "nanopores" to mean pores in the nanometer range, following other authors.
[33] K. S. W. Sing, D. H. Everett, R. A. W. Haul, L. Moscou, R. A. Pierotti, J. Rouquerol, and T. Siemieniewska, Pure Appl. Chem. **57**, 603 (1985).
[34] S. Patchkovskii, J. S. Tse, S. N. Yurchenko, L. Zhechkov, T. Heine, and G. Seifert, Proc. Natl. Acad. Sci. U.S.A. **102**, 10439 (2005).
[35] S. H. Vosko, L. Wilk, and M. Nusair, Can. J. Phys. **58**, 1200 (1980).
[36] C. Møller and M. S. Plesset, Phys. Rev. **46**, 618 (1934).
[37] B. Hammer, L. B. Hansen, and J. K. Nørskov, Phys. Rev. B **59**, 7413 (1999).
[38] http://dcwww.camp.dtu.dk/campos/Dacapo
[39] L. A. Girifalco and M. Hodak, Phys. Rev. B **65**, 125404 (2002).
[40] Y. Zhao and D. G. Truhlar, J. Chem. Theory Comput. **1**, 415 (2005).
[41] A. G. Donchev, J. Chem. Phys. **126**, 124706 (2007).
[42] A. Ferre-Vilaplana, J. Chem. Phys. **122**, 104709 (2005).
[43] S. B. Boys and F. Bernardi, Mol. Phys. **19**, 553 (1970).
[44] J. P. Perdew, J. A. Chevary, S. H. Vosko, K. A. Jackson, M. R. Pederson, D. J. Singh, and C. Fiolhais, Phys. Rev. B **46**, 6671 (1992).
[45] K. Tada, S. Furuya, and K. Watanabe, Phys. Rev. B **63**, 155405 (2001).